Alexandria Engineering Journal (2022) 61, 2220–2229

HOSTED BY

Alexandria University

Alexandria Engineering Journal

www.elsevier.com/locate/aej
www.sciencedirect.com

Free vibration of axially or transversely graded beams using finite-element and artificial intelligence

Sefa Yildirim *

Alanya Alaaddin Keykubat University, Mechanical Engineering Department, 07425 Alanya, Turkey

Received 6 April 2020; revised 8 June 2021; accepted 5 July 2021
Available online 24 July 2021

KEYWORDS

Free vibration;
Functionally-graded materials;
Beams;
Artificial neural network;
Finite-element method

Abstract The effect of grading direction on the natural frequencies of heterogeneous isotropic beams is investigated and the artificial neural network approach is conducted to estimate the free vibration characteristics. The two-dimensional beam is graded in axial or transverse direction according to the power-law form. An artificial neural network model has been developed to estimate relationship between material properties and model, grading direction, slenderness ratio as an input layer and natural frequencies obtained by Finite-Element method as an output layer. The Levenberg–Marquardt back-propagation method is used as a training algorithm. The novelty of this study is that it deals with the estimation of free vibration characteristics of beams made of functionally-graded material using aforementioned input layer for the first time. The proposed artificial neural network model can predict the natural frequencies without the need for a solution of any differential equation or time-consuming experimental processes. The results show that artificial intelligence techniques can be efficiently adopted to free vibration problems of functionally graded beams. The influence of grading direction on the natural frequency is also demonstrated.

1. Introduction

Functionally graded materials (FGMs), which are heterogeneous isotropic materials with varying mechanical properties in one, two or three directions, have been increasingly used in different applications such as vessels, aircrafts, energy storage devices so on. Due to the wide-spread application areas of FGMs, investigating the dynamic behavior of structural elements made of FGM is important. Salah et al. [1] have been investigated the buckling analysis of FGM plate subjected to hygrothermal and mechanical loads using a novel shear deformation theory where the shear correction factor is not needed. The effect of boundary conditions on the bending and free vibration characteristics of FGM plates is presented by Rahmani et al.[2]. In this study, the plate is assumed to be rested on a two-parameter elastic foundation and a four-unknown refined integral plate theory is implemented. Kaddari et al. [3] have proposed a quasi-three-dimensional hyperbolic shear deformation theory on the vibration and bending analyses of porous FGM plate where the simply-supported boundary conditions are taken into consideration. The some of the remaining recent works on dynamic analysis and solution methods of

* Corresponding author
E-mail address: sefa.yildirim@alanya.edu.tr.
Peer review under responsibility of Faculty of Engineering, Alexandria University.

https://doi.org/10.1016/j.aej.2021.07.004

FGMs presented by numerous researchers may be cited here [4–15].

The first study based on the free vibration of FGM beam has been conducted by Aydogdu and Taskin[16] using parabolic shear deformation theory, first-order shear deformation theory and exponential shear deformation theory. In their study, the beam is assumed to be transversely functionally graded (TFG). Li [17] has presented a unified method for the vibration problems of TFG Timoshenko and Euler-Bernoulli beams. The free and forced vibration of a TFG simply-supported beam under a concentrated moving harmonic load are examined by Simsek and Kocaturk [18] using Lagrange's equations. Simsek[19] has studied the effect of slenderness ratio, material variations and different shear deformation theories on fundamental frequencies of TFG beams. Sina et al.[20] have presented the analytical solution of the natural frequencies of TFG beams using first-order shear deformation theory. Celebi and Tutuncu[21] have evaluated the natural frequencies of transversely graded heterogeneous beams using plane elasticity approach. The differential transformation method is used by Wattanasakulpong and Ungbhakorn[22] to analyze free vibration characteristics of TFG beams resting general elastically end constraints. Analytical solutions of free vibration and bending of TFG beams based on the shear deformation theory are presented by Larbi et al.[23] where hyperbolic variations of the transverse shear strains and neutral surface position are taken into consideration. Lee and Lee [24] have studied the free vibration of heterogeneous beams using an exact transfer matrix method where beams are graded along the height of the beam cross section by a power-law distribution. Jing et al. [25] have examined the natural frequencies of TFG Timoshenko beams by ell-center finite volume method. In their study, Hamilton's principle is used to derive the general dynamic equations. The static response and free vibration behavior of FGM beam graded in transverse direction have been investigated by Khan et al. [26] using finite-element(FE) zigzag theory using various boundary conditions. Free vibration of heterogeneous beam is studied by Celebi et al. [27] using the complementary functions method. In their study, various grading functions and slenderness ratios are used to present the effectiveness of their proposed method. Ding et al. [28] have studied nonlinear vibration characteristics of TFG beams using Euler–Bernoulli beam theory and von Kármán's geometric nonlinearity. Lee and Lee [29] have presented the analytical method to evaluate the influence of shear deformation on the contribution rates of normal and shear strain energies to the free vibration.

On the free vibration of axially functionally graded (AFG) beams, several studies have been conducted. Huang and Li [30] have performed the free vibration analysis of non-uniform beam graded along the length of the beam cross section by transforming the forth-order governing equation to Fredholm integral equations. Analytical solutions of bending vibration of AFG one-layer and multilayered beams are presented by Murin et al. [31] where the shear force deformation effect and the effect of consistent mass distribution and mass inertia moment are considered. Alshorbagy et al. [32] have studied the free vibration of Euler–Bernoulli beam graded along the length or thickness. Shahba et al. [33] have investigated the free vibration behavior of non-uniform AFG beams using finite-element method. The transverse vibration of FGM beam graded in the axial direction is examined by Li et al. [34]. In their study, the beam is assumed to be non-uniform with exponentially decaying width. Tang et al. [35] have studied the natural frequency of tapered Timoshenko beams using different end conditions. Temel and Noori[36] and Aslan et al. [37] have investigated vibration behavior of laminated and homogeneous curved beams. Nikolic[38] is presented transverse and axial vibration studies of cantilever beam with a tip body using rigid element method. In his study, the Euler–Bernoulli beam is graded along the length direction and has a tapered cross-section. Noori et al. [39] have examined the in-plane free and forced vibration characteristics of AFG parabolic beam considering the shear deformation effect.

Artificial Neural Network(ANN) is one of the most popular artificial intelligence method for the prediction in different engineering areas. To this aspect, some studies related to various engineering areas are cited here. ANN model is constructed to predict the failure load values of single lap joints made of isotropic material by Tosun and Çalık [40] where it has been suggested that ANN can be used to eliminate the complex and time-consuming experimental work for the adhesive bonding problem of single lap joints. Yildirim et al. [41] have presented the artificial intelligence study on the estimation of vibration, noise and emission characteristics of internal combustion engine fueled by hydrogen enriched diesel. In their work, ANN and Adaptive Neuro-Fuzzy Inference Systems (ANFIS) are applied as the artificial intelligence techniques and it is concluded that ANN shows the better performance in the prediction of engine properties compared with ANFIS. Zgoul [42] has dealt with an ANN study in order to forecast true strain, true stress, strain rate, and modulus of elasticity of adhesives used in the single lap joints where ANN performance is measured by comparing with the experimental data. Zhang et al. [43] have presented a detailed review study on ANN as a forecasting tool in various field such as mathematics, aerospace and electrical engineering so on. Tosun et al. [44] have conducted a study to compare the efficiencies of linear regression (LR) and ANN approaches in the prediction of the overall engine outputs of biodiesel engine with the alcohol additive.

On the application of the artificial intelligence to the vibration problems are given hereafter. ANN and Adaptive Neuro-Fuzzy Inference Systems(ANFIS) have been used to determine the natural frequencies of cracked Timoshenko beams by Banerjee[45]. The free vibration analysis of FGM disk has been presented by Jodaei[46] using the combination of ANN and differential quadrature method. The application of ANN on the free vibration of basalt fiber reinforced polymer laminated non-uniform plates are presented by Altabey [47].

The plane free vibration analysis of heterogeneous beams results in the two coupled-second-order variable coefficient governing differential equations which should be reduced to a fourth-order variable coefficient differential equation. The necessary boundary conditions may be applied to the reduced-governing equation. Closed-form solution of this reduced-fourth-order equation is not possible except for simple material model. Therefore, numerical solution methods such as FEM, differential quadrature, Ritz or Galerkin must be applied to the governing equations to obtain the natural frequencies. The whole procedure contains complex mathematical manipulations. Another approach to obtain the free vibration characteristics of FGM beams requires to application of detailed experimental procedures which may be costly and laborious.

The present study deals with the free vibration analysis of TFG and AFG beams and the application of ANN to problems on hand. Natural frequencies obtained by Finite-Element Method (FEM) are given for FGM beams with different grading directions and number of layers. Effect of grading direction and efficiency of ANN on the free vibration of FGM beams are demonstrated. The main idea behind this study is to present an alternative approach on the determination of the free vibration behavior of functionally-graded beams. It is only needed to the limited knowledge of natural frequency data to train the algorithm. Using the proposed method, the model can readily be adapted for different material properties, boundary conditions and beam geometries as well. The ANN model presented in this work may be a proper approach to avoid the aforementioned mathematical operations and experiments by its easy-to-implement nature and providing high estimation capability for natural frequencies.

2. General properties of finite-element method

The idea behind the finite-element method is to obtain an approximate solution of boundary value problem where the treated body is assumed to be made of subdivisions called finite elements. Each element is considered to be coincident with other elements at the element boundary with nodes. The field representing the treated body is the domain of interest which may be displacements, stresses, velocities or temperatures depending on the type of problem. The unknown field variables of non-nodal points inside each subdivision are defined by the approximating functions or shape functions and field variables computed at the element nodes[48,49]. The following approximate relation representing the field variable at any point within the two-dimensional element is given below for purely illustration purposes:

$$\varphi(x,y) = \sum_{i=1}^{n} N_i \varphi_i \tag{1}$$

where n is the node number, N_i denote the shape functions and φ_i are the computed field variables at the nodal points.

The free vibration analysis of structures requires the solution of the following equation called as the eigenvalue problem:

$$\left([K] - \Omega^2[M]\right)\{\phi\} = \{0\} \tag{2}$$

where $\{\phi\}$ is the mode shape vector, Ω represents natural frequency, $[K]$ and $[M]$ denote the global stiffness and mass matrices producing by assembling the individual elements contributions with respect to their nodes.

3. Beam geometry and material model

A simply supported rectangular cross-section FGM beam of length L, depth h and unit width is depicted in Fig. 1. A Cartesian coordinate system is chosen and oriented at the center of the unbent beam where x-axis is taken as an axial direction and z-axis in the transverse direction. The beam is assumed to be under the conditions of plane-stress.

In this study, FGM beam made of two different constituents is used and two cases are considered. In the first case, the effective material properties of beam (Young's Modulus

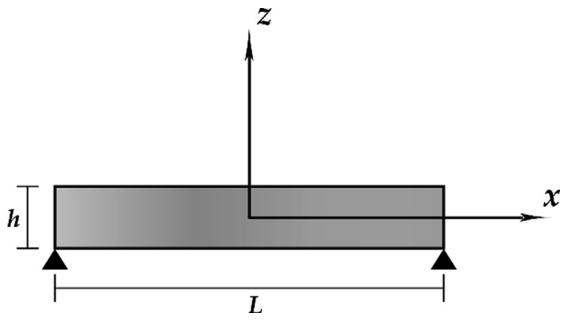

Fig. 1 Schematic of beam and coordinates.

E, Poisson's ratio$\nu$and densityρ) vary in the transverse (thickness) direction and in the second case, the material is assumed to be graded in the axial (length) direction. The effective material properties for TFG and AFG beam governed by power-law formulas are, respectively [19]:

$$P(z) = P_b + (P_t - P_b)\left(\frac{z}{h} + \frac{1}{2}\right)^{\lambda} \tag{3}$$

$$P(x) = P_l + (P_r - P_l)\left(\frac{x}{L} + \frac{1}{2}\right)^{\lambda} \tag{4}$$

where P is effective material properties, λ is power-law exponent, subscripts b or t denotes the bottom or top surface and subscripts l or r specifies left-end or right-end of the beam. Note that Eq.(3) and Eq.(4) represent the FGM beams graded in the transverse and axial directions, respectively.

The finite-element models of FGM beams are constructed by dividing the beam into numbers of homogeneous layers where each layer has different constant material properties. Material properties of homogeneous layers are defined by taking the average of values on both surfaces of layers for TFG beam and on both ends of layers for AFG beam using Eqs. (1–2). The nodes are coincident at the overlap regions of layers. The grading direction is, respectively, through the z-axis and x-axis for TFG and AFG beams. Two-dimensional structural solid element defined by 8-node with two degrees of freedom at each node (translations in the nodal $\times$ and z axes) is used and plane-stress element behavior is selected. The beam is assumed to be pinned–pinned boundaries due to the illustration of ANN effectiveness. However, any beam with different boundaries such as clamped–clamped or clamped-free can be evaluated.

4. Numerical FEM examples

In this section, several numerical results are given to compare the influence of grading direction of FGM beam on natural frequency and effectiveness of ANN model for the present type of problems. Two different material pair for FGM are selected. The first material pair for the FGM is composed of two different metals namely Steel and Aluminum. The beam is Steel rich at the bottom and left-end and Al rich at the top and right-end for TFG and AFG, respectively. The idea behind the selection of these two metallic materials as constituents of FGM is to validate the FEM results with those given in the literature [17,19]. The second material pair contains metal and ceramic

constituent as Aluminum and Zirconia. It is assuemed that the bottom and left-end of the beam are Al rich and the top and right-end are ZrO_2 rich for TFG and AFG, respectively. The material properties for the constituents given in Table 1.

The FEM codes are written by MATLAB and implemented in ANSYS Mechanical APDL. PLANE183 two-dimensional structural solid element which has quadratic displacement behavior and is well suited to modeling irregular meshes is selected. For the detailed element type information used in this paper, it is referred to reference[50]. The beams are divided into 2000, 3000 and 4000 equal elements depending on L/h ratio.

5. Artificial neural network model

ANN idea is based on simulating the functions of biological neurons. The general ANN structure contains three layers, namely, an input layer, a hidden layer, and an output layer. The detailed information about the theoretical background and working principle of ANN can be found in the literature [40,41]. In the present study, the input layer is composed of grading direction (TFG or AFG), the effective material properties of material pairs(E_1,v_1,$\rho_1$and E_2,v_2,ρ_2), grading index λ and slenderness ratio L/h. Here subscripts 1 and 2 denote, depending on the grading direction, the bottom or left-end and top or right-end of beam. The input data are selected for $N = 50$ and FEM results with $\lambda = 0.1$ and $\lambda = 10$ which are not given in the Results and Discussions section to prevent the redundancy also considered. The total neuron numbers in hidden layer are defined as 18 using trial–error method. Levenberg–Marquardt (LM) algorithm is chosen as a learning algorithm. LM is proven to be the most efficient algorithm for training of moderate-sized feed-forward neural networks (up to several hundred weights). The idea behind the LM is to serve as an intermediate optimization algorithm between the Gauss–Newton (GN) method and gradient descent algorithm, and overcome the limitations of each of those techniques. The LM algorithm obtained by modification of GN method is given below[51,52]:

$$\Delta w_k = -\left[J^T(w_k).J(w_k) + \mu_k I\right]^{-1} J^T(w_k)e(w_k) \tag{5}$$

where w, J and e are weight of simulated neuron, Jacobian matrix and the error vector, respectively. The parameter μ is multiplied by a factor $\eta > 1$ when a step increases the function and the parameter is divided by η when the function decreases. In this work, the initial parameter $\mu$and factor η, respectively, are 0.01 and 2.

The output layer is made of first five fundamental natural frequencies (Ω_1-Ω_5) of beam. The randomly selected 75% of data provided to ANN model are used for training and the remaining are picked for testing. Note that a complete set of data composed of first to fifth natural frequencies is given for training hence the correlation is not only between frequencies with the same mode number but also all frequencies with different mode numbers. The ANN structure used in this study is depicted in Fig. 2.

Table 1 Properties of selected constituents.

	Steel	Al	ZrO_2
$E\,(GPa)$	210	70	200
v	0.3	0.3	0.22
$\rho\,(kg/m^3)$	7850	2702	5700

The convergency tests of ANN results are done by the mean average percent error (MAPE, %) and the regression correlation coefficient (R) given by Eqs. (4–5):

$$MAPE(\%) = \frac{100}{n}\sum_{i=1}^{n}\left(\frac{T_i - O_i}{T_i}\right) \tag{6}$$

$$R = \left(1 - \left(\sum_{i=1}^{n}(T_i - O_i)/\sum_{i=1}^{n}O_i^2\right)\right)^{0.5} \tag{7}$$

where T and O are target and output values, respectively. The smaller MAPE values (MAPE $\leq 10\%$) and R^2 values close to 1 show that the prediction performance of constructed ANN architecture is quite high for the prescribed problem.

6. Results and discussions

As a first step, natural frequencies of TFG and AFG beams are obtained for the first material (Steel-Al) pair using different power-law exponent ($\lambda = 0$, 0.5, 1, 2, and 5) and results are tabulated in Tables 2-6. In the tables, Ω_i denotes the natural frequency, subscript i denotes the mode number and N denotes the number of layers to emulate the FGM behavior. For the isotropic beam (Table 2), the natural frequencies are very close to each other and increasing number of layers for the both case (TFG and AGB) does not affect the natural frequencies considerable, as expected. The results given in the present study for pure Al ($\lambda = 0$) and $\lambda = 1$ have a great agreement with those of Şimşek[4] and Li[2]. As it can be seen from the tables, natural frequencies of AFG beams are generally higher than TFG beams except for pure Al beam and the effect of power-law exponents on natural frequencies of beams is higher for TFG beams than AFG beams for the first natural frequency. The unit of frequencies in the results is the Hertz (Hz).

The free vibration analysis of FGM beam with Al and ZrO_2 constituents are performed and results are given in Tables 7–12. As it can be seen from the tables, the results have different

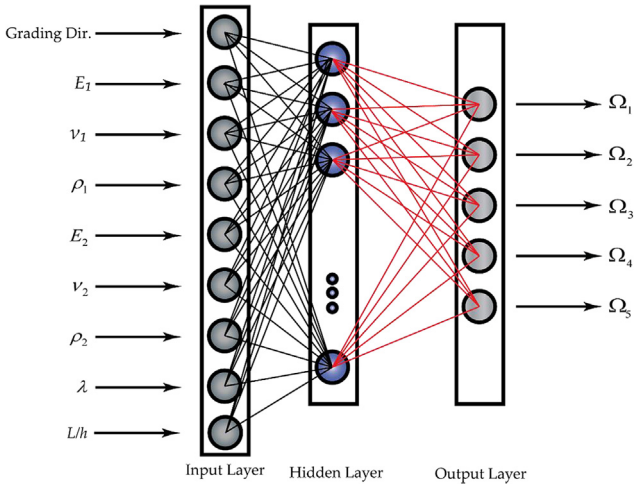

Fig. 2 Illustration of ANN architecture for predictions.

Table 2 The effect of number of layers on natural frequencies of AFG and TFG beam (Steel-Al).

$\lambda = 0$	$N = 10$		$N = 20$		$N = 50$		$N = 100$	
Ω	AFG	TFG	AFG	TFG	AFG	TFG	AFG	TFG
Ω_1	1053.023714	1053.023714	1053.023712	1053.023712	1053.023714	1053.023712	1053.023712	1053.023712
Ω_2	3488.812344	3488.812373	3488.812344	3488.812352	3488.812343	3488.812349	3488.812454	3488.812350
Ω_3	6441.506129	6441.506205	6441.506130	6441.506181	6441.506132	6441.506179	6441.506418	6441.506163
Ω_4	9553.136036	9553.136219	9553.136041	9553.136223	9553.136029	9553.136227	9553.136657	9553.136228
Ω_5	12614.737320	12614.73764	12614.737338	12614.737222	12614.737339	12614.737280	12614.737484	12614.737238

Table 3 The effect of number of layers on natural frequencies of AFG and TFG beam (Steel-Al).

$\lambda = 0.5$	$N = 10$		$N = 20$		$N = 50$		$N = 100$	
Ω	AFG	TFG	AFG	TFG	AFG	TFG	AFG	TFG
Ω_1	1051.114539	1048.782605	1051.385588	1048.496917	1051.436460	1048.062902	1051.440907	1047.913868
Ω_2	3523.570614	3474.598984	3524.000443	3475.386160	3523.776651	3474.835088	3523.691079	3474.554408
Ω_3	6503.803544	6411.966384	6506.244050	6416.070972	6505.650231	6416.377715	6505.375052	6416.166244
Ω_4	9637.748940	9501.544952	9645.989731	9510.776904	9645.606521	9512.787994	9645.149998	9512.819124
Ω_5	12663.055656	12618.771585	12662.616449	12634.577389	12666.922784	12639.030252	12668.342345	12639.448854

Table 4 The effect of number of layers on natural frequencies of AFG and TFG beam (Steel-Al).

$\lambda = 1$	$N = 10$		$N = 20$		$N = 50$		$N = 100$	
Ω	AFG	TFG	AFG	TFG	AFG	TFG	AFG	TFG
Ω_1	1047.605300	1028.075115	1047.772520	1027.529247	1047.816892	1027.375088	1047.823116	1027.353018
Ω_2	3521.768416	3436.710241	3521.724939	3435.678099	3521.709042	3435.383418	3521.706836	3435.341114
Ω_3	6507.746692	6384.768294	6506.583928	6383.954401	6506.268493	6383.715112	6506.224741	6383.680503
Ω_4	9655.529877	9505.677564	9652.273833	9505.574134	9651.423240	9505.529910	9651.305765	9505.523001
Ω_5	12737.159430	12667.278285	12723.192364	12668.120168	12719.372047	12668.342543	12718.832987	12668.373785

Table 5 The effect of number of layers on natural frequencies of AFG and TFG beam (Steel-Al).

$\lambda = 2$	$N = 10$		$N = 20$		$N = 50$		$N = 100$	
Ω	AFG	TFG	AFG	TFG	AFG	TFG	AFG	TFG
Ω_1	1047.829040	1015.753772	1047.859711	1014.401288	1047.862843	1014.018275	1047.863096	1013.963402
Ω_2	3507.130957	3419.406105	3505.415196	3416.319837	3504.918407	3415.433860	3504.847108	3415.306481
Ω_3	6498.306467	6386.937677	6491.891203	6383.257911	6490.113180	6382.174751	6489.860789	6382.018038
Ω_4	9655.859062	9545.103613	9641.469601	9541.760789	9637.625561	9540.730425	9637.084216	9540.579564
Ω_5	12747.147625	12754.633243	12719.707735	12752.190761	12712.069870	12751.362749	12710.987456	12751.238869

tendencies for different material pairs therefore the material properties have a crucial role on the free vibration characteristics for FGM beam even for the same material model. Also, it is shown that a linear decrease in the natural frequency is observed for the AFG beam with the increase of power-law exponent. Similar behavior is observed for the TFG beam up to $\lambda = 5$. When the power-law exponent is equal to 5, an increase in the natural frequency is seen and the natural frequency decreases again with the increase of exponent parameter. The effect of slenderness ratio (L/h) is investigated and results are tabulated in Tables 13 and 14 for $N = 50$. Increasing the slenderness ratio decreases the natural frequency considerably. The results and efficiency of ANN application to the problem on hand will be discussed hereafter.

The ANN performance for estimating natural frequencies of TFG and AFG beams is quite well. The correlation of predicted and FEM results for the first natural frequency is given in Fig. 3 and the correlation coefficient is calculated R^2 as 0.997261. The predicted results are in a very good agreement with FEM results for the second natural frequency so that the R^2 is 0.999316 as illustrated in Fig. 4. The result depicted in Fig. 5 yields the correlation coefficient R^2 of 0.999166 for

Table 6 The effect of number of layers on natural frequencies of AFG and TFG beam (Steel-Al).

$\lambda = 5$	$N = 10$		$N = 20$		$N = 50$		$N = 100$	
Ω	AFG	TFG	AFG	TFG	AFG	TFG	AFG	TFG
Ω_1	1054.460329	1020.135865	1054.505874	1019.010196	1054.488850	1018.692329	1054.484933	1018.646809
Ω_2	3487.292071	3437.165213	3483.126752	3434.165600	3481.791203	3433.289863	3481.591183	3433.163308
Ω_3	6467.780154	6425.402998	6450.954184	6420.957048	6445.931826	6419.597808	6445.195797	6419.398938
Ω_4	9628.343760	9609.515708	9590.003402	9604.170221	9578.948238	9602.438543	9577.345927	9602.181360
Ω_5	12686.814612	12848.864526	12617.780581	12843.137892	12597.499808	12841.141648	12594.564705	12840.839755

Table 7 The effect of number of layers on natural frequencies of AFG and TFG beam (Al-ZrO_2).

$\lambda = 0$	$N = 10$		$N = 20$		$N = 50$		$N = 100$	
Ω	AFG	TFG	AFG	TFG	AFG	TFG	AFG	TFG
Ω_1	1230.665062	1230.665065	1230.665063	1230.665062	1230.665058	1230.665062	1230.665071	1230.665062
Ω_2	4098.948419	4098.948450	4098.948413	4098.948424	4098.948417	4098.948425	4098.948475	4098.948425
Ω_3	7599.427370	7599.427483	7599.427371	7599.427402	7599.427364	7599.427419	7599.427510	7599.427424
Ω_4	11304.060172	11304.060409	11304.060182	11304.060419	11304.060212	11304.060400	11304.060489	11304.06038
Ω_5	15060.135902	15060.136321	15060.135872	15060.136695	15060.135844	15060.136426	15060.136362	15060.136455

Table 8 The effect of number of layers on natural frequencies of AFG and TFG beam (Al-ZrO_2).

$\lambda = 0.5$	$N = 10$		$N = 20$		$N = 50$		$N = 100$	
Ω	AFG	TFG	AFG	TFG	AFG	TFG	AFG	TFG
Ω_1	1185.863401	1158.953969	1187.092901	1161.118743	1187.630540	1162.469435	1187.764538	1162.842861
Ω_2	3937.631786	3892.050179	3942.497160	3897.283980	3945.640336	3900.620292	3946.553488	3901.562567
Ω_3	7290.449965	7261.031526	7293.177936	7267.842971	7299.614453	7272.353399	7301.882930	7273.673147
Ω_4	10847.912880	10848.127037	10835.687634	10855.145630	10844.124586	10860.071678	10848.113742	10861.590254
Ω_5	14282.046027	14498.473945	14247.394004	14504.761455	14263.968508	14509.574680	14273.100982	14511.175132

Table 9 The effect of number of layers on natural frequencies of AFG and TFG beam (Al-ZrO_2).

$\lambda = 1$	$N = 10$		$N = 20$		$N = 50$		$N = 100$	
Ω	AFG	TFG	AFG	TFG	AFG	TFG	AFG	TFG
Ω_1	1154.203667	1136.116800	1154.355631	1135.555374	1154.395072	1135.396831	1154.400484	1135.374134
Ω_2	3861.022730	3804.762281	3860.755436	3803.670446	3860.674718	3803.358848	3860.662807	3803.314118
Ω_3	7143.309148	7084.731055	7141.420336	7083.820881	7140.904474	7083.553943	7140.831178	7083.515359
Ω_4	10611.501976	10573.192660	10606.647434	10572.987358	10605.383161	10572.912246	10605.205473	10572.900798
Ω_5	13919.702971	14123.102928	13904.179993	14123.865627	13899.715066	14124.057883	13899.076795	14124.084545

Table 10 The effect of number of layers on natural frequencies of AFG and TFG beam (Al-ZrO_2).

$\lambda = 2$	$N = 10$		$N = 20$		$N = 50$		$N = 100$	
Ω	AFG	TFG	AFG	TFG	AFG	TFG	AFG	TFG
Ω_1	1115.949919	1125.977560	1115.728763	1126.265059	1115.663911	1126.347987	1115.654376	1126.359921
Ω_2	3756.885332	3731.033853	3756.730925	3731.743171	3756.679500	3731.954324	3756.671597	3731.984943
Ω_3	6940.502797	6894.884834	6940.933491	6895.998260	6941.018260	6896.345129	6941.029027	6896.395966
Ω_4	10295.410711	10240.405763	10297.043637	10241.995596	10297.367358	10242.516529	10297.409582	10242.593688
Ω_5	13409.690444	13372.231368	13402.598312	13362.236693	13400.591534	13359.450944	13400.304647	13359.053486

Table 11 The effect of number of layers on natural frequencies of AFG and TFG beam (Al-ZrO_2).

$\lambda = 5$	$N = 10$		$N = 20$		$N = 50$		$N = 100$	
Ω	AFG	TFG	AFG	TFG	AFG	TFG	AFG	TFG
Ω_1	1078.870985	1135.352477	1078.460349	1137.303382	1078.337581	1137.855341	1078.319666	1137.934399
Ω_2	3613.317842	3690.805825	3612.357656	3695.193892	3612.051979	3696.450313	3612.006567	3696.630819
Ω_3	6689.196578	6724.800861	6688.430149	6730.405051	6688.091103	6732.054544	6688.038050	6732.293154
Ω_4	9924.983960	9891.483029	9925.270498	9897.457762	9924.985779	9899.312249	9924.933411	9899.583807
Ω_5	12991.195751	12134.588712	12981.461266	12108.355273	12978.626426	12101.036178	12978.218318	12099.991894

Table 12 The effect of material parameter on natural frequencies of AFG and TFG beam (Al-ZrO_2).

$L/h = 6$	$\lambda = 0$		$\lambda = 0.5$		$\lambda = 1$		$\lambda = 2$		$\lambda = 5$	
Ω	AFG	TFG	AFG	TFG	AFG	TFG	AFG	TFG	AFG	TFG
Ω_1	572,683794	572,683802	554,858776	539,677642	539,552755	527,409570	520,203208	525,070378	501,0154893	533,871214
Ω_2	2068,271321	2068,271327	1999,662739	1958,691835	1955,316320	1911,913681	1900,480281	1889,392822	1827,840691	1895,516521
Ω_3	4098,948417	4098,948446	3962,087461	3900,620312	3864,807677	3803,358870	3755,179514	3731,954345	3622,910179	3696,450331
Ω_4	6397,213402	6397,213550	6161,404689	6111,797480	6020,627797	5954,784402	5845,729661	5810,412136	5643,836329	5696,191093
Ω_5	8822,339657	8822,340091	8488,972529	8454,985474	8291,744754	8233,704460	8045,914563	8000,709745	7767,916925	7780,877218

Table 13 The effecst of material parameter on natural frequencies of AFG and TFG beam (Al-ZrO_2).

$L/h = 10$	$\lambda = 0$		$\lambda = 0.5$		$\lambda = 1$		$\lambda = 2$		$\lambda = 5$	
Ω	AFG	TFG	AFG	TFG	AFG	TFG	AFG	TFG	AFG	TFG
Ω_1	211,585178	211,585171	205,480942	199,102761	199,854493	194,645711	192,408229	194,208989	184,927919	198,262100
Ω_2	810,901946	810,901946	786,645488	764,847343	768,872683	747,298540	746,657747	742,980398	718,078966	753,578082
Ω_3	2368,919238	2368,919238	2378,403095	2308,574277	2302,181339	2266,878698	2136,256724	2212,585715	1946,172452	2139,331010
Ω_4	2834,829622	2834,829696	2740,538840	2690,078752	2676,964334	2624,615806	2599,649752	2585,939856	2511,967915	2580,392027
Ω_5	4734,864174	4734,864166	4659,471448	4613,817036	4513,126505	4529,800344	4331,936834	4419,966377	4141,721971	4271,981964

Ω_3. The best estimation performance of constructed ANN has been observed in Fig. 6 which shows the results for Ω_4 with the correlation coefficient R^2 of 0.999755. The ANN predictions for the Ω_5 illustrated in Fig. 7 yield the correlation coefficient R^2 of 0.999293. Also, the MAPE (%) values of the ANN algorithm for the first five natural frequencies, respectively, are

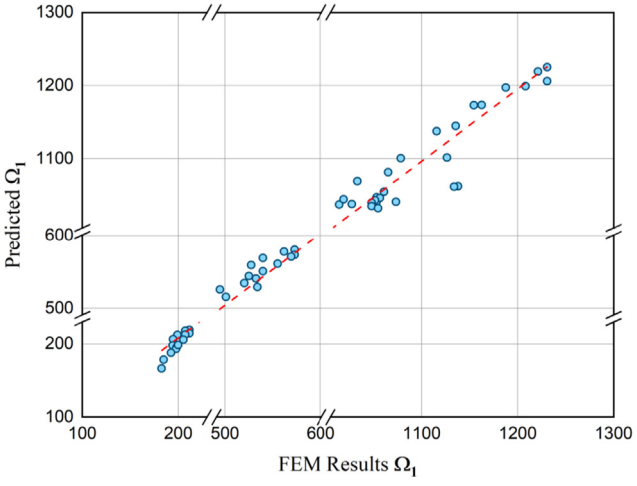

Fig. 3 Correlation between FEM and ANN results of Ω_1.

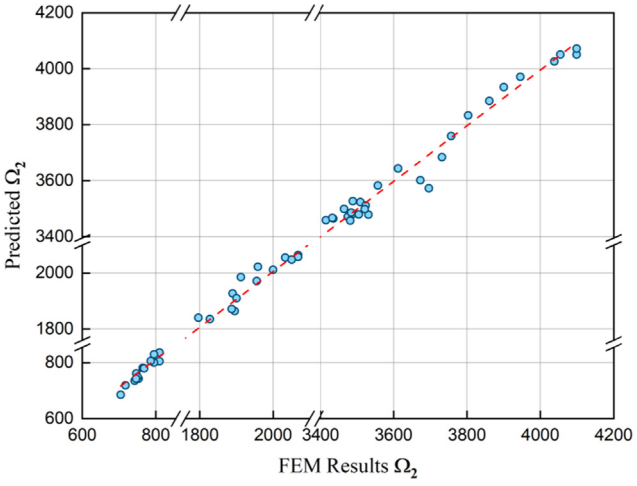

Fig. 4 Correlation between FEM and ANN results of Ω_2.

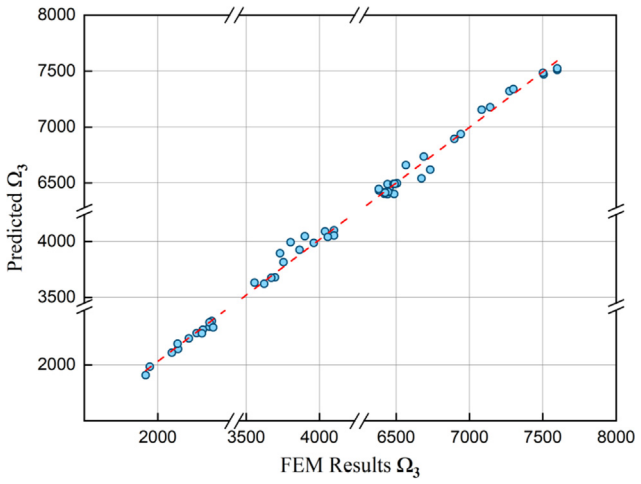

Fig. 5 Correlation between FEM and ANN results of Ω_3.

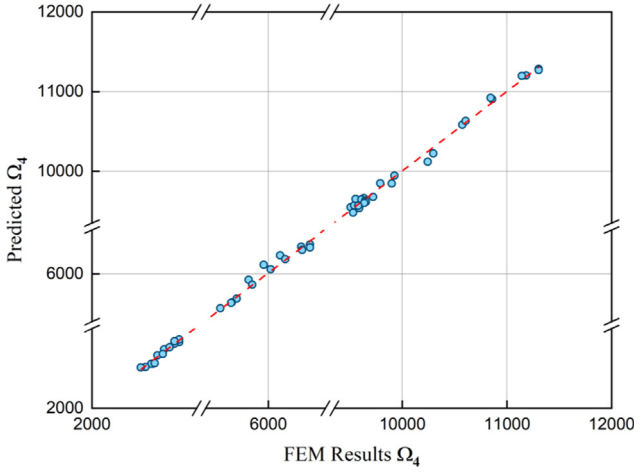

Fig. 6 Correlation between FEM and ANN results of Ω_4.

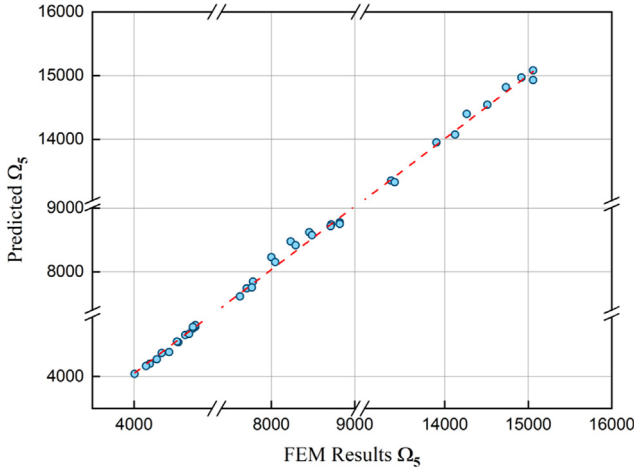

Fig. 7 Correlation between FEM and ANN results of Ω_5.

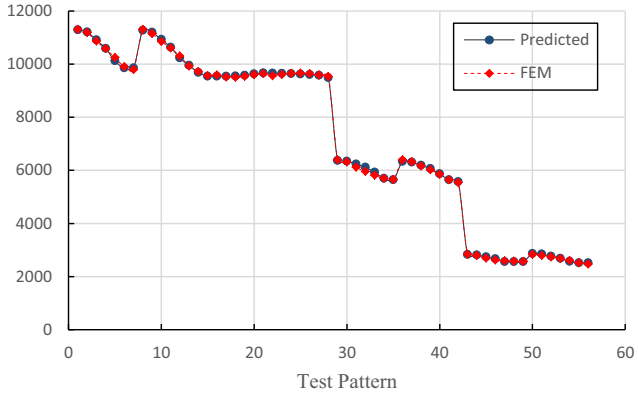

Fig. 8 Comparison of FEM and ANN results for Ω_4.

2.38796, 1.15325, 0.95685, 0.65229 and 0.75306. It is showed that the performance testing methods are consisted with each other and obtained results are very robust. The comparison of ANN and FEM results of best estimation performance (Ω_4) is illustrated in Fig. 8 to emphasize the efficiency of algorithm. As seen from the results, ANN has showed excellent estimation performance for free vibration behavior of FGM beams and it can be used to avoid making complex and time-consuming mathematical manipulations and experiments.

7. Conclusions

The present paper uses the FEM to evaluate the influences of grading direction on the free vibration behavior of FGM beam. The validation FEM results are done by using data available in the literature. Also, the artificial intelligence method (ANN) is used to predict the natural frequencies. The effectiveness of ANN structure and convergency of results are tested using the mean average percent error and the regression correlation coefficient methods. The results show that ANN can be considered as an alternative method to overcome difficult mathematical calculations and experiments for the free vibration analysis of heterogeneous beams. The followings are the summarized results of the analysis:

- For the first material pair (Al-St), using an axial grading generally increases the natural frequency and the influence of power-law exponent on the first fundamental natural frequency is higher for the transverse grading compared with the axial grading.
- For the second material pair (Al-ZrO_2), increasing the power-law exponent decreases the natural frequency for the both grading procedure except for $\lambda = 5$ case of transverse grading.
- The selection of material pairs has a pivotal role in the free vibration characteristic of AFG or TFG beam since the variation of natural frequencies shows different tendencies even for the same grading procedure.
- The correlation coefficient R^2 values of ANN algorithm are 0.997261, 0.999316, 0.999166, 0.999755 and 0.999293 for the first five natural frequencies, respectively. Similarly, the MAPE (%) values, respectively, are 2.38796, 1.15325, 0.95685, 0.65229 and 0.75306. The performance testing

results indicate that both testing methods are consistent and accurate for the ANN application on free vibration analysis.

- The best estimation performance is developed for forth natural frequency Ω_4 with highest R^2 value and lowest MAPE (%) value as 0.999755 and 0.65229, respectively.

Funding

This research received no specific grant from any funding agency in the public, commercial, or not-for-profit sectors.

Declaration of Conflicting Interests

The author declared no potential conflicts of interest with respect to the research, authorship, and/or publication of this article.

References

[1] S. Refrafi, Bousahla A. A., Bouhadra A., Menasria A., Bourada F., Tounsi A., et al., Effects of hygro-thermo-mechanical conditions on the buckling of FG sandwich plates resting on elastic foundations, Comput. Concr. 25(2020) 311-25.

[2] M. C. Rahmani, Kaci A., Bousahla A. A., Bourada F., Tounsi A., Bedia E., et al., Influence of boundary conditions on the bending and free vibration behavior of FGM sandwich plates using a four-unknown refined integral plate theory, Comput. Concr. 25(2020) 225-44.

[3] M. Kaddari, Kaci A., Bousahla A. A., Tounsi A., Bourada F., Tounsi A., et al., A study on the structural behaviour of functionally graded porous plates on elastic foundation using a new quasi-3D model: bending and free vibration analysis, Comput. Concr. 25(2020) 37-57.

[4] A. Tounsi, Al-Dulaijan S., Al-Osta M. A., Chikh A., Al-Zahrani M., Sharif A., et al., A four variable trigonometric integral plate theory for hygro-thermo-mechanical bending analysis of AFG ceramic-metal plates resting on a two-parameter elastic foundation, Steel Compos. Struct. 34(2020) 511-24.

[5] A. Boussoula, Boucham B., Bourada M., Bourada F., Tounsi A., Bousahla A. A., et al., A simple nth-order shear deformation theory for thermomechanical bending analysis of different configurations of FG sandwich plates, Smart Struct. Syst. 25 (2020) 197-218.

[6] M. Balubaid, Tounsi A., Dakhel B., Mahmoud S., Free vibration investigation of FG nanoscale plate using nonlocal two variables integral refined plate theory, Comput. Concr. 24 (2019) 579-86.

[7] F. Y. Addou, Meradjah M., Bousahla A. A., Benachour A., Bourada F., Tounsi A., et al., Influences of porosity on dynamic response of FG plates resting on Winkler/Pasternak/Kerr foundation using quasi 3D HSDT, Comput. Concr . 24(2019) 347-67.

[8] M. Medani, Benahmed A., Zidour M., Heireche H., Tounsi A., Bousahla A. A., et al., Static and dynamic behavior of (FG-CNT) reinforced porous sandwich plate using energy principle, Steel Compos. Struct. 32(2019) 595-610.

[9] S. Boutaleb, Benrahou K. H., Bakora A., Algarni A., Bousahla A. A., Tounsi A., et al., Dynamic analysis of nanosize FG rectangular plates based on simple nonlocal quasi 3D HSDT, Adv. Nano Res. 7(2019) 191.

[10] S. I. Tahir, Chikh A., Tounsi A., Al-Osta M. A., Al-Dulaijan S. U., Al-Zahrani M. M., Wave propagation analysis of a ceramic-metal functionally graded sandwich plate with different porosity distributions in a hygro-thermal environment, Compos. Struct. 269(2021) 114030.

[11] X. Huang, H. Hao, K. Oslub, M. Habibi, A. Tounsi, Dynamic stability/instability simulation of the rotary size-dependent functionally graded microsystem, Eng. Comput. (2021).

[12] S. Alimirzaei, Mohammadimehr M., Tounsi A., Nonlinear analysis of viscoelastic micro-composite beam with geometrical imperfection using FEM: MSGT electro-magneto-elastic bending, buckling and vibration solutions, Struct Eng Mech. 71(2019) 485-502.

[13] B. Karami, Janghorban M., Tounsi A., Galerkin's approach for buckling analysis of functionally graded anisotropic nanoplates/ different boundary conditions, Eng. Comput. 35(2019) 1297-316.

[14] A. Shariati, M. Habibi, A. Tounsi, H. Safarpour, M. Safa, Application of exact continuum size-dependent theory for stability and frequency analysis of a curved cantilevered microtubule by considering viscoelastic properties, Eng. Comput. (2020) 1–20.

[15] M. Hussain, Naeem M. N., Taj M., Tounsi A., Simulating vibration of single-walled carbon nanotube using Rayleigh-Ritz's method, Adv. Nano Res. 8(2020) 215-28.

[16] M. Aydogdu, Taskin V., Free vibration analysis of functionally graded beams with simply supported edges, Mater. Des. 28 (2007) 1651-6.

[17] X.-F. Li, A unified approach for analyzing static and dynamic behaviors of functionally graded Timoshenko and Euler-Bernoulli beams, J. Sound Vib. 318 (2008) 1210–1229.

[18] M. Şimşek, Kocatürk T., Free and forced vibration of a functionally graded beam subjected to a concentrated moving harmonic load, Compos. Struct. 90(2009) 465-73.

[19] M. Şimşek, Fundamental frequency analysis of functionally graded beams by using different higher-order beam theories, Nucl. Eng. Des. 240 (2010) 697–705.

[20] S. Sina, Navazi H., Haddadpour H., An analytical method for free vibration analysis of functionally graded beams, Mater. Des. 30(2009) 741-7.

[21] K. Celebi, Tutuncu N., Free vibration analysis of functionally graded beams using an exact plane elasticity approach, Proc. Inst. Mech. Eng. Pt. C J. Mechan. Eng. Sci. 228(2014) 2488-94.

[22] N. Wattanasakulpong, Ungbhakorn V., Free vibration analysis of functionally graded beams with general elastically end constraints by DTM, World J. Mech. 2(2012) 297.

[23] L. O. Larbi, Kaci A., Houari M. S. A., Tounsi A., An Efficient Shear Deformation Beam Theory Based on Neutral Surface Position for Bending and Free Vibration of Functionally Graded Beams, Mech. Based Des. Struct. Mach. 41(2013) 421-33.

[24] J. W. Lee, Lee J. Y., Free vibration analysis of functionally graded Bernoulli-Euler beams using an exact transfer matrix expression, Int. J. Mech. Sci. 122(2017) 1-17.

[25] L.-l. Jing, Ming P.-j., Zhang W.-p., Fu L.-r., Cao Y.-p., Static and free vibration analysis of functionally graded beams by combination Timoshenko theory and finite volume method, Compos. Struct. 138(2016) 192-213.

[26] A. A. Khan, Naushad Alam M., Wajid M., Finite element modelling for static and free vibration response of functionally graded beam, Lat. Am. J. Solids Struct. 13(2016) 690-714.

[27] K. Celebi, Yarimpabuc D., Tutuncu N., Free vibration analysis of functionally graded beams using complementary functions method, Arch. Appl. Mech. 88(2018) 729-39.

[28] J. Ding, Chu L., Xin L., Dui G., Nonlinear vibration analysis of functionally graded beams considering the influences of the rotary inertia of the cross section and neutral surface position, Mech. Based Des. Struct. Mach. 46(2018) 225-37.

[29] J. W. Lee, Lee J. Y., Contribution rates of normal and shear strain energies to the natural frequencies of functionally graded shear deformation beams, Compos. B. Eng. 159(2019) 86-104.

[30] Y. Huang, Li X.-F., A new approach for free vibration of axially functionally graded beams with non-uniform cross-section, J. Sound Vib. 329(2010) 2291-303.
[31] J. Murin, Aminbaghai M., Kutiš V., Exact solution of the bending vibration problem of FGM beams with variation of material properties, Eng. Struct. 32(2010) 1631-40.
[32] A. E. Alshorbagy, Eltaher M. A., Mahmoud F. F., Free vibration characteristics of a functionally graded beam by finite element method, Appl. Math. Model. 35(2011) 412-25.
[33] A. Shahba, Attarnejad R., Hajilar S., Free vibration and stability of axially functionally graded tapered Euler-Bernoulli beams, Shock Vib. 18(2011) 683-96.
[34] X.-F. Li, Kang Y.-A., Wu J.-X., Exact frequency equations of free vibration of exponentially functionally graded beams, Appl. Acoust. 74(2013) 413-20.
[35] A.-Y. Tang, Wu J.-X., Li X.-F., Lee K., Exact frequency equations of free vibration of exponentially non-uniform functionally graded Timoshenko beams, Int. J. Mech. Sci. 89 (2014) 1-11.
[36] A.R. Noori, B. Temel, On the vibration analysis of laminated composite parabolic arches with variable cross-section of various ply stacking sequences, Mech. Adv. Mater. Struct. 27 (2019) 1658–1672.
[37] Temel B., T. A. Aslan, Noori A. R., In-plane vibration analysis of parabolic arches having a variable thickness, Int. J. Dyn. Control. 92(2021) 1-12.
[38] A. Nikolić, Free vibration analysis of a non-uniform axially functionally graded cantilever beam with a tip body, Arch. Appl. Mech. 87 (2017) 1227–1241.
[39] A. R. Noori, Aslan T. A., Temel B., An efficient approach for in-plane free and forced vibrations of axially functionally graded parabolic arches with nonuniform cross section, Compos. Struct. 200(2018) 701-10.
[40] E. Tosun, Calık A., Failure load prediction of single lap adhesive joints using artificial neural networks, Alex. Eng. J. 55(2016) 1341-6.
[41] S. Yıldırım, Tosun E., Çalık A., Uluocak İ., Avşar E., Artificial intelligence techniques for the vibration, noise, and emission characteristics of a hydrogen-enriched diesel engine, Energ Source Part A. 41(2019) 2194-206.
[42] M.H. Zgoul, Use of artificial neural networks for modelling rate dependent behaviour of adhesive materials, Int. J. Adhes. Adhes. 36 (2012) 1–7.
[43] E. Tosun, Aydin K., Bilgili M., Comparison of linear regression and artificial neural network model of a diesel engine fueled with biodiesel-alcohol mixtures, Alex. Eng. J. 55(2016) 3081-9.
[44] G. Zhang, Patuwo B. E., Hu M. Y., Forecasting with artificial neural networks:: The state of the art, Int. J. Forecast. 14(1998) 35-62.
[45] A. Banerjee, Pohit G., Panigrahi B., Vibration Analysis and Prediction Natural Frequencies of Cracked Timoshenko Beam by Two Optimization Techniques-Cascade ANN and ANFIS, Mater. Today Proc. 4(2017) 9909-13.
[46] A. Jodaei, Jalal M., Yas M., Free vibration analysis of functionally graded annular plates by state-space based differential quadrature method and comparative modeling by ANN, Compos. B. Eng. 43(2012) 340-53.
[47] W.A. Altabey, Prediction of natural frequency of basalt fiber reinforced polymer (FRP) laminated variable thickness plates with intermediate elastic support using artificial neural networks (ANNs) method, J. Vibroeng. 19 (2017) 3668–3678.
[48] D.V. Hutton, Fundamentals of Finite Element Analysis, first ed., McGraw-Hill, New York, 2004.
[49] S.S. Bhavikatti, Finite Element Analysis, first ed., New Age International, New Delhi, 2005.
[50] M.K. Thompson, Thompson J, Butterworth-Heinemann, M. ANSYS mechanical APDL for finite element analysis, 2017.
[51] C. Lv, Xing Y., Zhang J., Na X., Li Y., Liu T., et al., Levenberg–Marquardt Backpropagation Training of Multilayer Neural Networks for State Estimation of a Safety-Critical Cyber-Physical System, IEEE Trans. Industr. Inform. 14(2018) 3436-46.
[52] B. G. Kermani, Schiffman S. S., Nagle H. T., Performance of the Levenberg–Marquardt neural network training method in electronic nose applications, Sens. Actuators B Chem. 110(2005) 13-22.